Table S1

Mutation	Mitochondrial Morphology
$Mfn1^{R83W}$	Fragmented, short tubules
$Mfn1^{H107R}$	Fragmented, aggregated fragments
$Mfn1^{T109A}$	Fragmented
$Mfn1^{A143V}$	Short tubules
$Mfn1^{H144R}$	Fragmented
$Mfn1^{D178A}$	Fragmented
$Mfn1^{F202L}$	Highly elongated, perinuclear collapse
$Mfn1^{P230A}$	Reticular
$Mfn1^{V252G}$	Fragmented, short tubules, some reticular
$Mfn1^{Q255R}$	Fragmented
$Mfn1^{R259H}$	Short tubules, reticular
$Mfn1^{F263Y}$	Reticular

Functional screen of Mfn1 GTPase domain mutant variants. Description of the mitochondrial morphology of GTPase domain mutant variants generated in Mfn1-eGFP and expressed in $Mfn1^{-/-}$ $Mfn2^{+/+}$ cells by retroviral transduction.

A

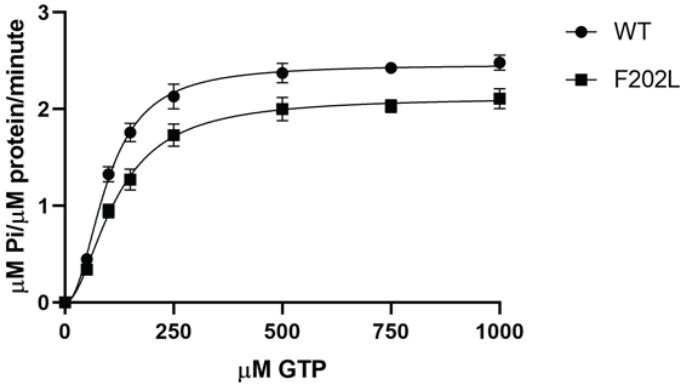

B

	WT	F202L
Vmax	2.461	2.123
h	2.119	1.884
Khalf	96.51	116.6

Figure S1
Kinetic analysis of GTP hydrolysis of $Mfn1_{IM}C$ and $Mfn1^{F202L}{}_{IM}C$**. (A)** A representative kinetic plot fit to an allosteric sigmoidal equation is shown. **(B)** Kinetic parameters for $Mfn1_{IM}C$ and $Mfn1^{F202L}{}_{IM}C$.

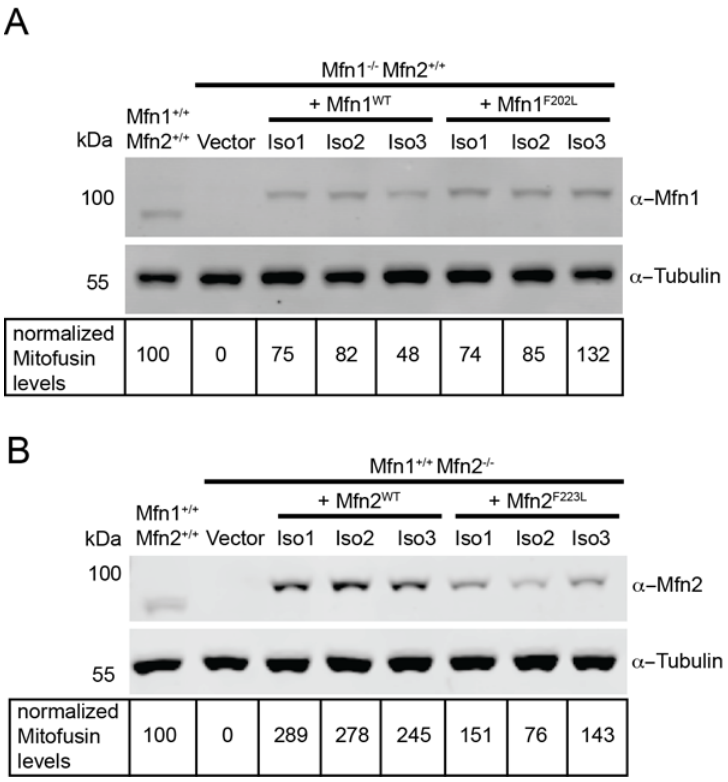

Figure S2

Mitofusin-FLAG protein expression in MEF clonal populations. **(A)** Whole-cell lysates prepared from indicated cell lines were subjected to SDS-PAGE and immunoblotting with α-Mfn1 and α-Tubulin. Protein loading was normalized to Tubulin and for each clonal population, the relative amount of Mfn1-FLAG to endogenous Mfn1 is listed below. **(B)** Whole-cell lysates prepared from indicated cell lines were subjected to SDS-PAGE and immunoblotting with α-Mfn2 and α-Tubulin. Protein loading was normalized to Tubulin and for each clonal population, the relative amount of Mfn2-FLAG to endogenous Mfn2 is listed below.

Figure S3

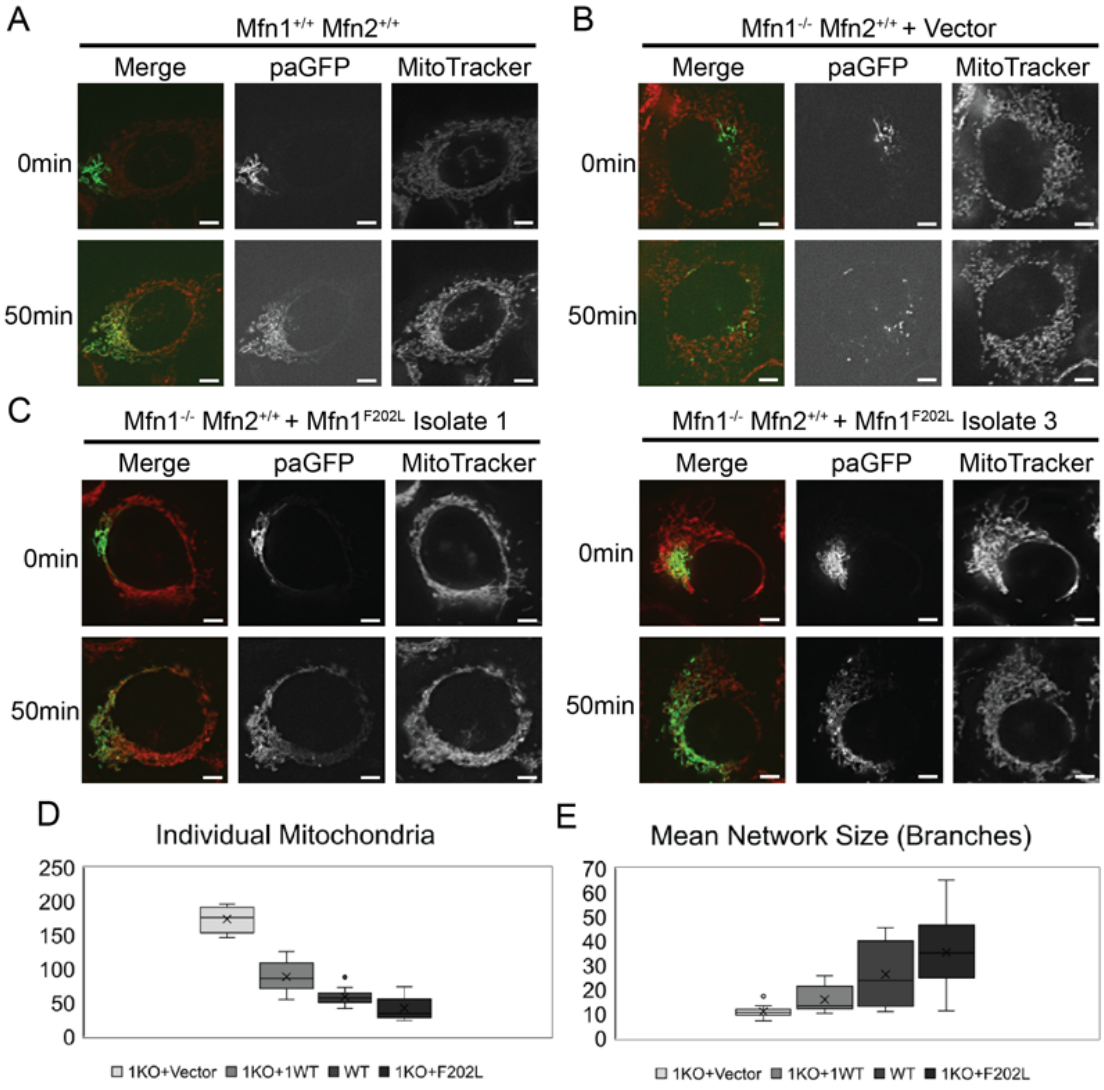

Figure S3

Mitochondrial connectivity and fusion as measured by redistribution of GFP. Wildtype (A) or clonal populations of Mfn1-null cells transduced with empty vector (B) or Mfn1^{F202L} (C) trasduced with mitochondrial matrix-targed photoactivatible-GFP (mt-paGFP) were labeled with MitoTracker Red CMXRos and visualized by fluorescence microscopy. A small region of the cell that contained mitochondria (approximately 1 micron square) was activated using a 405 nm laser (t=0 min) and the same cell was re-imaged 50 minutes later (t-50 min). The Pearson's correlation co-efficient for red and green pixels was calculated as a measure of GFP spreading through the mitochondrial network. For wildtype controls, the co-efficient was 0.32 at t=0 and 0.627 at t=50; for empty vector, the co-efficient was 0.09 at t=0 and 0.077 at t=50; for F202L isolate 1, the co-efficient was 0.315 at t=0 and 0.603 at t=50; for F202L isolate 3, the co-efficient was 0.459 at t=0 and 0.653 at t=50. Mitochondrial network analysis was performed with the Image J MiNa plugin to assess the number of individual mitochondria (D) and the mean network

size (E) in wildtype, or clonal populations of Mfn1-null cells transduced with empty vector or expressing Mfn1F202L.

Figure S4

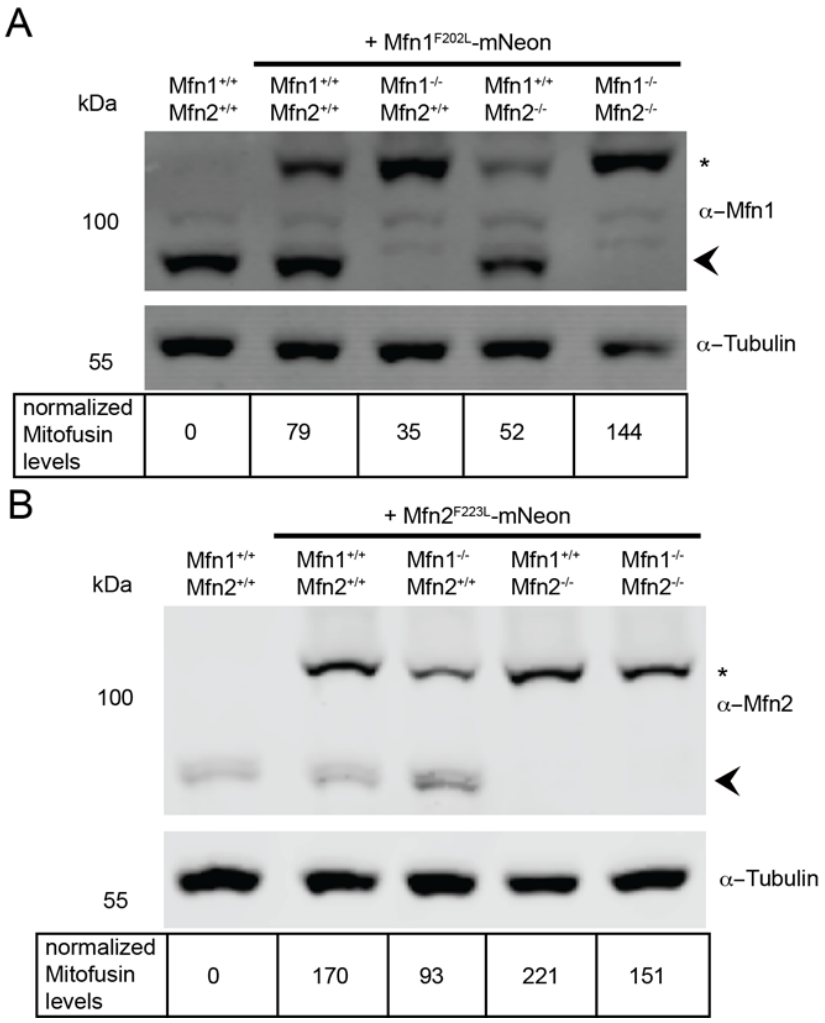

Figure S4
Mitofusin-mNeon protein expression in MEFs of the indicated genotype. **(A)** Whole-cell lysates prepared from indicated cell lines expressing Mfn1^{F202L}-mNeon were subjected to SDS-PAGE and immunoblotting with α-Mfn1and α-Tubulin. Protein loading was normalized to Tubulin and for each cell line, the relative amount of Mfn1-mNeon to endogenous Mfn1 is listed below. **(B)** Whole-cell lysates prepared from indicated cell lines expressing Mfn2^{F223L}-mNeon were subjected to SDS-PAGE and immunoblotting with α-Mfn2 and α-Tubulin. Protein loading was normalized to Tubulin and for each cell line, the relative amount of Mfn2-mNeon to endogenous Mfn2 is listed below. Arrowhead indicated endogenous Mitofusin and asterisk indicates Mitofusin with C-terminal mNeonGreen.

Figure S5

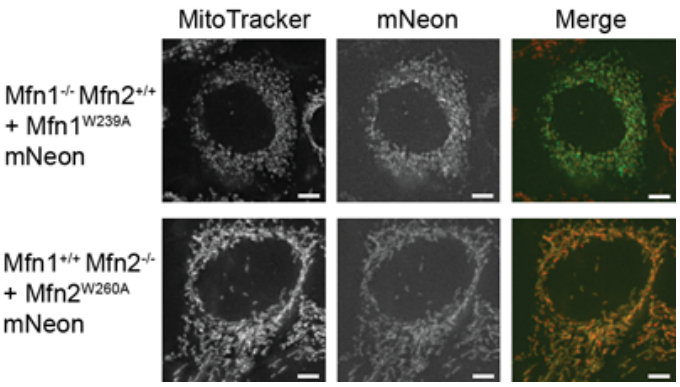

Figure S5
Functional assessment of Mfn1^{W239A} and Mfn2^{W260A}. Representative images of Mfn1-null cells expressing Mfn1^{W239A}-mNeon and Mfn2-null cells expressing Mfn2^{W260A}-mNeon following viral transduction. Mitochondria were labeled with MitoTracker Red CMXRos and visualized by fluorescence microscopy. Images represent maximum intensity projections. Scale bars are 5 μM.

Figure S6

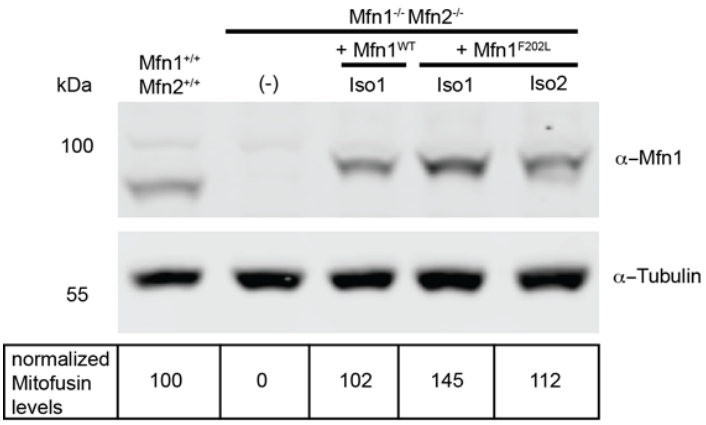

normalized Mitofusin levels	100	0	102	145	112

Figure S6
Mfn1-FLAG and Mfn1^{F202L}-FLAG protein expression in Mfn1/2-null clonal populations. Whole-cell lysates prepared from indicated cell lines were subjected to SDS-PAGE and immunoblotting with α-Mfn1 and α-Tubulin. Protein loading was normalized to Tubulin and for each clonal population, the relative amount of Mfn1-FLAG to endogenous Mfn1 is listed below.

Figure S7

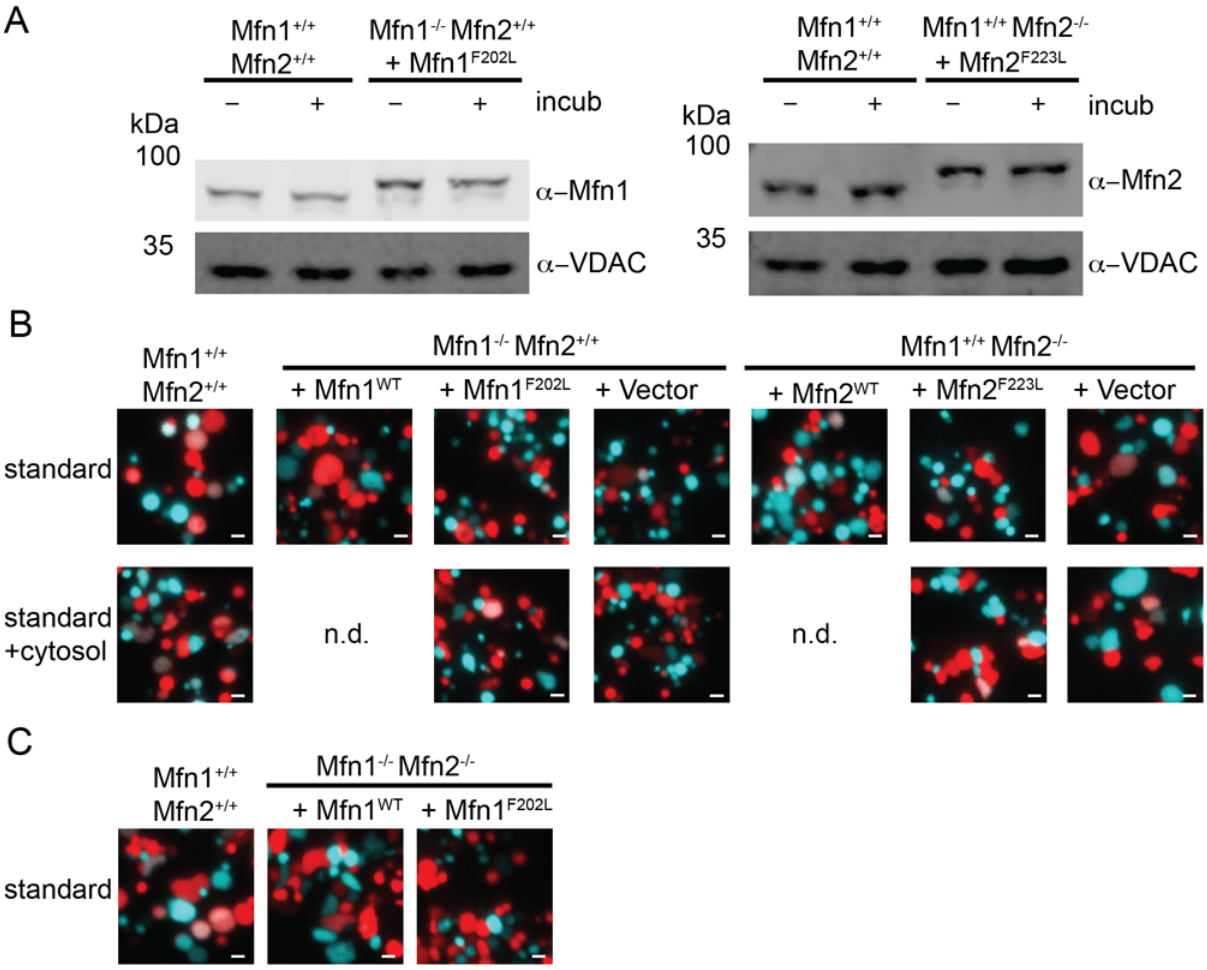

Figure S7

Mitofusin protein stability and mitochondrial morphology in vitro. **(A)** To assess the protein stability under the in vitro fusion conditions, isolated mitochondria were either left untreated (-) or were subject to in vitro fusion conditions (+) prior to analysis by SDS-PAGE and immunoblotting with α-Mfn1, α-Mfn2 and, α-VDAC. **(B)** Representative images from in vitro fusion reactions described in Figure 5A & B. **(C)** Representative images from in vitro fusion reactions described in Figure 5D.

Figure S8

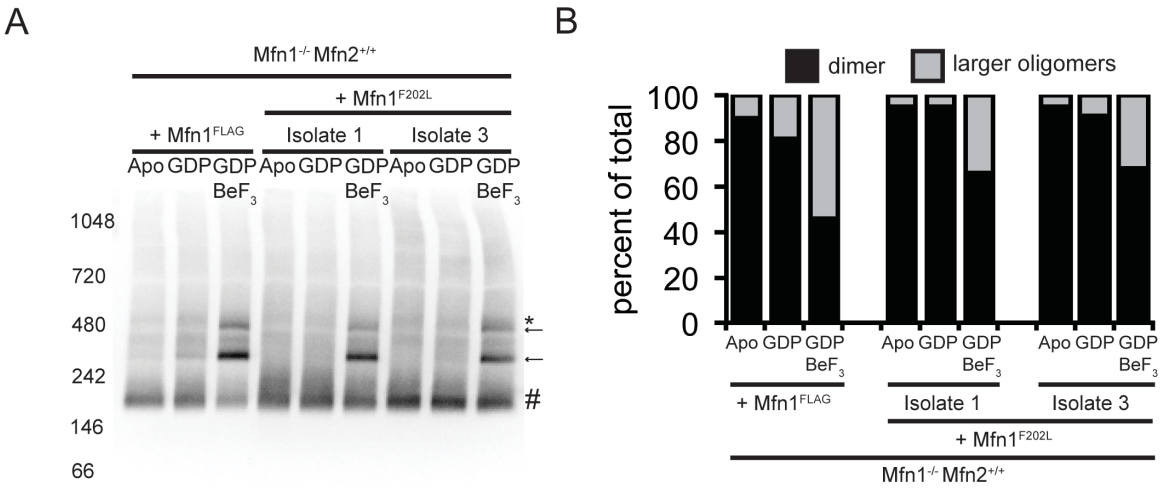

Figure S8
Mfn1^{F202L} has impaired nucleotide dependent assembly. **(A)** Mitochondria were isolated from indicated cell lines, either left untreated, or were incubated with the indicated nucleotide condition prior to lysis, and were then subjected to BN-PAGE and immunoblotted with α-FLAG. # denotes the predicted dimer state, arrows denote the larger oligomeric species and * denotes a non-specific band. **(B)** The percentage of total protein in the smaller oligomeric state (#)(predicted dimer) and the higher oligomeric states (arrows) for each condition in (A) is represented in the bar graph.

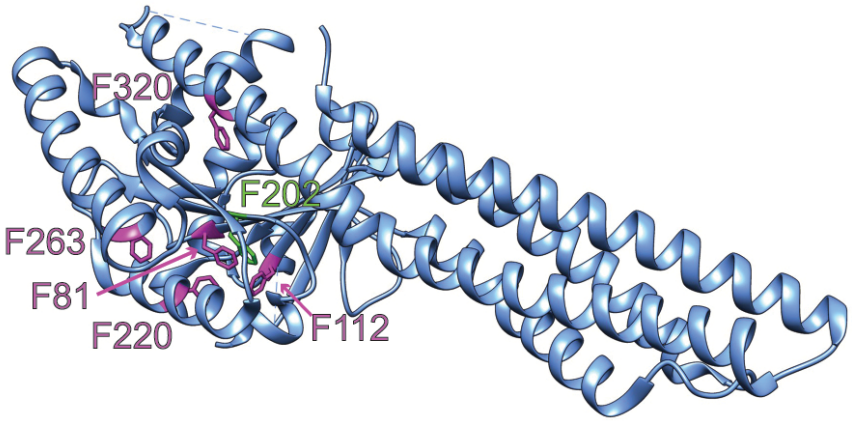

Figure S9
Aromatic network that includes F202 as well as F81, F112, F219, F220, F263 and F320 (PDB 5G04).